Scientific Reports

https://doi.org/10.1038/s41598-026-38188-1

Article in Press

Platelet-rich plasma promotes cellular recovery from nicotine-induced toxicity via autophagy modulation

Received: 24 October 2025

Accepted: 29 January 2026

Published online: 09 February 2026

Cite this article as: Vérièpe-Salerno J., Cancela J.A., Vischer S. *et al.* Platelet-rich plasma promotes cellular recovery from nicotine-induced toxicity via autophagy modulation. *Sci Rep* (2026). https://doi.org/10.1038/s41598-026-38188-1

Julie Vérièpe-Salerno, José Antonio Cancela, Solange Vischer, Antoine Turzi, Muriel Cuendet, Catherine Giannopoulou & Sarah Berndt

Platelet-Rich Plasma promotes cellular recovery from nicotine-induced toxicity via autophagy modulation

Julie Vérièpe-Salerno[1,2], José Antonio Cancela[3], Solange Vischer[4], Antoine Turzi[4], Muriel Cuendet[1,2], Catherine Giannopoulou[3] and Sarah Berndt[4,5*]

[1] School of Pharmaceutical Sciences, University of Geneva, Geneva, Switzerland

[2] Institute of Pharmaceutical Sciences of Western Switzerland, University of Geneva, Geneva, Switzerland

[3] Division of Regenerative Dental Medicine and Periodontology, University Clinics of Dental Medicine, Faculty of Medicine, University of Geneva, Geneva, Switzerland

[4] Regen Lab SA, 1052 Le Mont-sur-Lausanne, Switzerland

[5] Faculty of Medicine, Geneva University, 1205 Geneva, Switzerland

* Corresponding author Sarah Berndt, sberndt@regenlab.com

Keywords: nicotine- platelet rich plasma- autophagy- periodontitis

Abstract

Chronic exposure to nicotine significantly exacerbates periodontitis, a prevalent inflammatory disease, by inducing cellular processes such as autophagy and inflammation in gingival fibroblasts. Current therapies often fail to fully address these cellular alterations in smokers, highlighting a need for innovative therapeutic and generative approaches. This study explores the therapeutic potential of Platelet-Rich Plasma (PRP), a blood-derived product, to modulate nicotine-induced biological activities in primary gingival fibroblasts, particularly in the case of periodontitis in smokers. Gingival fibroblasts were treated with increasing concentrations of nicotine, which led to senescence and autophagy. Nicotine at high concentrations triggered cellular vacuolization, a decrease in metabolism, viability and proliferation. Concomitant cell treatment with 10% PRP reverse nicotine effects and significantly cell migration potential. In Caenorhabditis elegans, PRP reduced the nicotine-induced autophagic activity. A screening of gingival fibroblast secretome revealed a modulation of autophagy-related cytokines in response to nicotine and/or PRP. The findings demonstrate that PRP could effectively inhibit nicotine-induced autophagy gingival fibroblasts, offering insights into its possible use as a therapeutic tool for managing periodontitis in smokers. The study underscores the potential of PRP in altering disease progression by modulating key cellular processes affected by smoking.

Introduction

Periodontitis is an inflammatory disease characterized by microbially associated host-mediated inflammation that results in loss of periodontal attachment. Bacterial biofilm formation initiates gingival inflammation. Periodontitis occurs when the balance between the microbial biofilm and the host is lost, due to dysbiosis that induces a perturbation of the host homeostasis in susceptible individuals. Current evidence supports that periodontitis is a multifactorial disease, as several systemic and environmental factors may modify the host's susceptibility to periodontitis and the disease's extent, severity, progression, and response to therapy [1].

Tobacco smoking has been identified as a major risk factor for periodontitis. The damaging effect of smoking has been shown in several epidemiological and clinical studies. Furthermore, studies on the potential mechanisms by which smoking tobacco may predispose to periodontal disease have been conducted. It appeared that smoking may affect the vasculature, the humoral immune system, and the cellular immune and inflammatory systems [2]. For example, neutrophil migration and chemotaxis in the periodontal tissues were impaired in smokers, the vasculature was decreased, and several functions of gingival and periodontal ligament fibroblast were impaired [3-5].

Nicotine is highly harmful to oral cells and significantly contributes to the progression of periodontal disease. It exhibits cytotoxic effects on oral epithelial cells and fibroblasts, which are critical for maintaining the structure and function of gum tissues. Nicotine reduces cell viability and impairs the proliferation of these cells, limiting the body's ability to repair damaged tissues. Moreover, it intensifies the inflammatory response within the oral cavity, leading to the release of pro-inflammatory cytokines that cause further tissue and bone damage. Another key issue is that nicotine induces vasoconstriction, which restricts blood flow to the gums, thereby reducing oxygen and nutrient delivery. This impaired circulation slows down healing processes and increases susceptibility to infections [6].

In the context of periodontitis, nicotine accelerates alveolar bone loss, which compromises tooth support. This is primarily driven by nicotine's effect on osteoclast activity, promoting the breakdown of bone tissue. Additionally, nicotine hampers the immune system's ability to manage bacterial plaque, which allows periodontal pathogens to proliferate unchecked, thereby worsening the disease. It also alters the oral microbial environment, favoring the growth of harmful bacteria associated with periodontitis. Furthermore, nicotine interferes with collagen production, which is essential for gum and bone integrity. It reduces collagen synthesis and increases its degradation, leading to weaker gums and the formation of deeper periodontal pockets [7].

Nicotine also significantly impacts wound healing and tissue regeneration in periodontal procedures. The substance reduces fibroblast activity, impairs blood supply, and generally delays the healing of periodontal tissues following interventions like scaling and root planning. These combined effects highlight why individuals who smoke or use nicotine products are at a considerably higher risk for developing severe periodontitis and face greater challenges in managing the disease.

Autophagy is a cellular process that allows cells to degrade and recycle their own components, helping to maintain cell homeostasis and survival during stress conditions. The term "autophagy"

comes from Greek, meaning "self-eating." It involves the formation of a double-membrane structure called the autophagosome, which engulfs damaged organelles, proteins, and other cellular debris. The autophagosome then fuses with a lysosome, forming an autolysosome, where the acidic environment and lysosomal enzymes work together to degrade the contents, which are then either recycled for energy or repurposed to build new cellular components. Autophagy also plays a role in immune responses, development, and adaptation to nutrient deprivation. Dysregulation of autophagy is linked to various diseases, including cancer, neurodegenerative disorders like Alzheimer's disease or amyotrophic lateral sclerosis, and metabolic diseases such as diabetes [8].
Periodontal treatment aims to reduce the inflammatory response, decrease disease progression, and ideally, regenerate lost periodontal structures. Thus, in addition to meticulous mechanical cleaning of the tooth surfaces, several regenerative techniques have been introduced for the treatment of periodontitis to remove the bacterial deposits (plaque and calculus). Among these, platelet-rich plasma (PRP) has been proposed due to its antibacterial properties, and its role in homeostasis and wound healing [9]. Several *in vitro* studies have shown a significant effect of PRP on several functions including osteoblast and fibroblast proliferation and differentiation [10-13]. Recent clinical research confirmed that using PRP as an agent for a periodontal wound increased the concentration of growth factor locally, thus enhancing the healing outcome [14]. Platelet concentrates (PCs) are easily obtained from the patient blood by centrifugation and are widely used for sinus floor elevation, alveolar ridge preservation, periodontal bone defects, guided bone regeneration, and treatment of gingival recession. Autologous PCs are ideal for this purpose because they have a high concentration of platelets, growth factors, and cytokines [15].

The aim of the present research project was to investigate the influence of PRP on various cellular functions of nicotine-treated gingival fibroblasts (GF). We showed that the PRP can partially compensate for the negative effect of nicotine on the cells of the periodontium, thus it could be recommended in the treatment of periodontitis in smokers in a preventive or curative approach.

Results

Nicotine induces morphological changes in human gingival fibroblasts that are counterbalanced by PRP treatment

At 48 h exposure, low amount of nicotine (25, 100 ng/ml) did not induce visible morphological changes in GF, whereas the two highest doses of nicotine (250 and 500 ng/ml) brought an increase in vacuolization. The addition of 10% PRP for another 48 h reversed the phenotype and led to an increase in cell number (Figure 1).

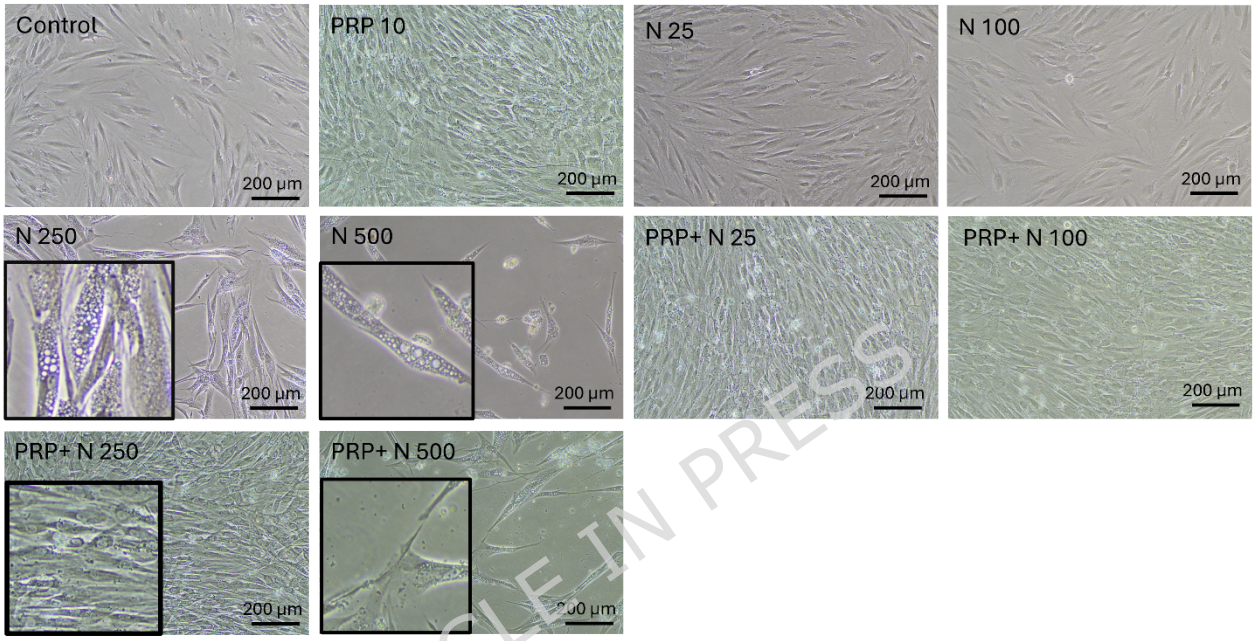

Figure 1. **Nicotine-induced phenotypic modifications in GF are reversed by PRP treatment.** Increasing concentrations of nicotine (25, 100, 250, 500 ng/ml) were added to GF culture for 4 days. At Day 2, PRP was added in different conditions. Bright-field pictures at 10x. Boxes are zoomed-in magnifications.

High doses nicotine exposure led to significant alterations in the metabolic activity and viability of GF, which were partially reversed by PRP

Nicotine induced a loss of more than 50 % of the metabolic activity after 96 h treatment with 500 ng/ml as evaluated by WST-1 incorporation (Figure 2A). In control condition with heparin, the metabolic activity was not significatively different than in control condition without heparin showing that 2UI/ml heparin had no effect on the GF. Hence, heparin alone controls were not shown in the following experiments. Heparin-added 10 % PRP without nicotine induced a potent effect on cell proliferation, metabolism and viability (Figure 2A, 2B, 2D, 2F).

Consistently, the intracellular ATP production measured via Cell Titer Glow assay (Figure 2B) was also significantly decreased by about 30 % in cells treated with the highest concentration of nicotine, indicating impaired cellular energy metabolism. PRP totally restored ATP levels following nicotine exposure, including at 500 ng/ml (Figure 2B). Fluorescent microscopy of

calcein-stained cells (Figure 2C) further supported these findings, with visibly reduced green fluorescence in high nicotine-exposed conditions reflective of compromised cell viability.

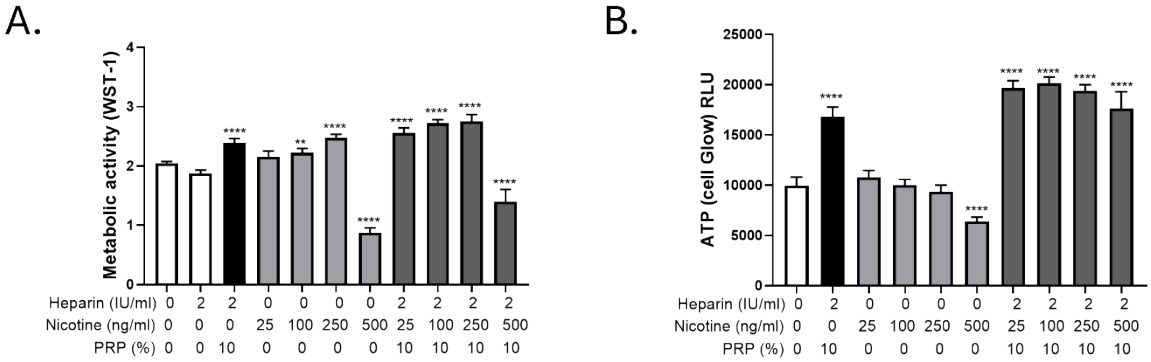

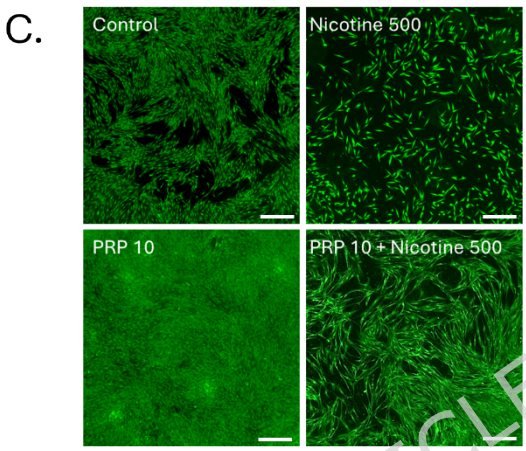

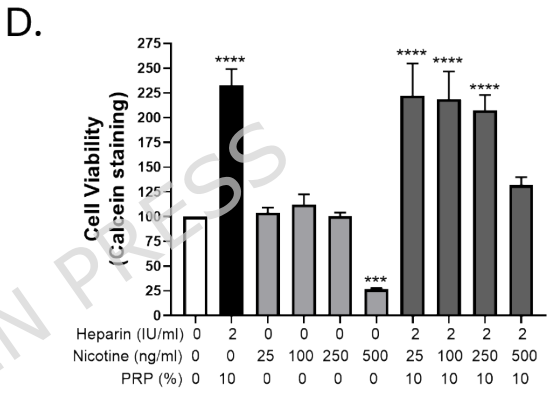

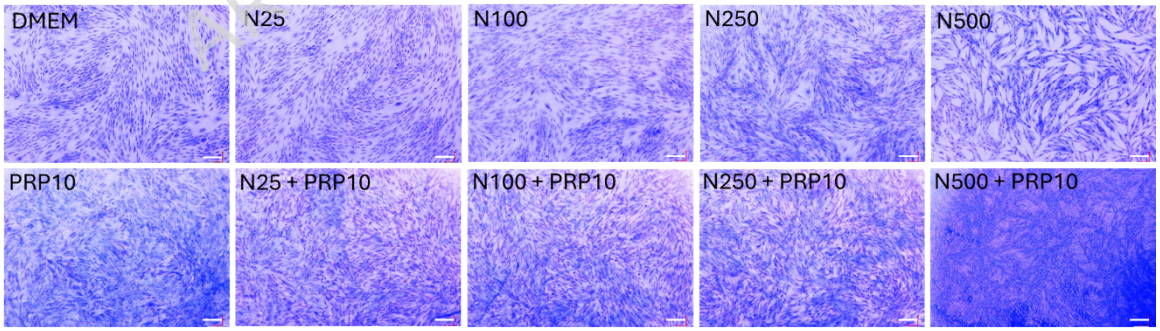

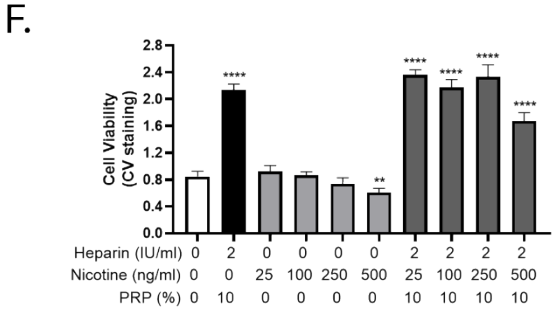

Figure 2. **Nicotine impaired GF metabolic activity and viability, mitigated by PRP.** Increasing concentrations of nicotine (25, 100, 250, 500 ng/ml) were added to GF culture for 4 days. At Day 2, PRP was added in the annotated conditions. Heparin alone was used as the control for PRP conditions. A. Metabolic activity of the cells assessed by WST-1 incorporation (n=8 per experimental condition). B. Total intracellular ATP production assessed by Cell Titer Glow (n=8 per experimental condition). C. Calcein microscopic acquisitions at 4x (scale bar= 200 µm). D. Cell viability is assessed by calcein incorporation followed by fluorescent measurement (n=3 per experimental condition). E. Crystal violet for cellular viability assessment, pictures taken at 10x magnification. (scale bar= 200 µm) F. Quantification of crystal violet dye release by absorbance measurement (n=4 per experimental condition). Data presented in this figure are from representative experiments from at least 3 independent repetitions. **p < 0.01, ***p < 0.001 and ***p <0,0001, PRP alone and nicotine doses alone were compared to control condition, while the combinations of nicotine and PRP were compared to the nicotine alone respective concentrations.

Quantitative calcein incorporation (Figure 2D) confirmed 75 % of decrease in viable cells compared to untreated controls (p < 0.001). In parallel, crystal violet (CV) staining (Figure 2E) demonstrated reduced cell density in nicotine-treated cultures, with absorbance quantification (Figure 2F) corroborating a significant loss in cell number of about 25 %. Notably, the addition of 10% PRP after two days of nicotine exposure rescued both metabolic (about 20 % for the highest concentration of nicotine, Figure 2A and total rescue for ATP level (Figure 2B), and viability (total rescue for calcein and CV staining, Figure D and F) metrics. These data indicate that high dose nicotine negatively impacted GF metabolic function and survival, while PRP exerted a protective effect, enhancing recovery from nicotine-induced cytotoxic stress.

PRP restored cell migration impaired by nicotine exposure in GF.

Representative images from the Ibidi chamber assay (Figure 3A) with visibly wider gaps remaining in control groups and more complete closure in nicotine alone, PRP alone and nicotine-PRP-rescued conditions. Together, these results indicate that 10% PRP exerted a synergistic effect together with nicotine (250 ng/ml) on fibroblast migration, highlighting its potential role in supporting wound healing in nicotine-compromised environments. PRP and nicotine together significantly improved wound closure, suggesting a pro-migratory effect. Wound healing quantification (Figure 3B) demonstrated a slight but significant increase in gap closure in nicotine-treated cells (250 ng/ml) and in 10% PRP treated cells after 24 h compared to control conditions, indicating that nicotine enhanced GF migration at that concentration. At 10% PRP, fibroblast migration increases due to growth factor–driven activation of pro migratory pathways (PI3K/AKT, ERK, Rac1/Rho) and enhanced cytoskeletal remodeling. When 250 ng/mL nicotine is added, the cells appear to show a hormetic, low dose stimulatory effect: moderate nicotine can activate nicotinic acetylcholine receptors, briefly boosting ERK/Src signaling and calcium dependent cytoskeletal dynamics. In PRP primed cells, this additional stimulus may potentiate PRP driven pathways, producing a supralinear increase in motility. At this

concentration, nicotine likely acts as a mild, adaptive stress cue, further promoting a repair□oriented, migratory phenotype rather than inhibiting it.

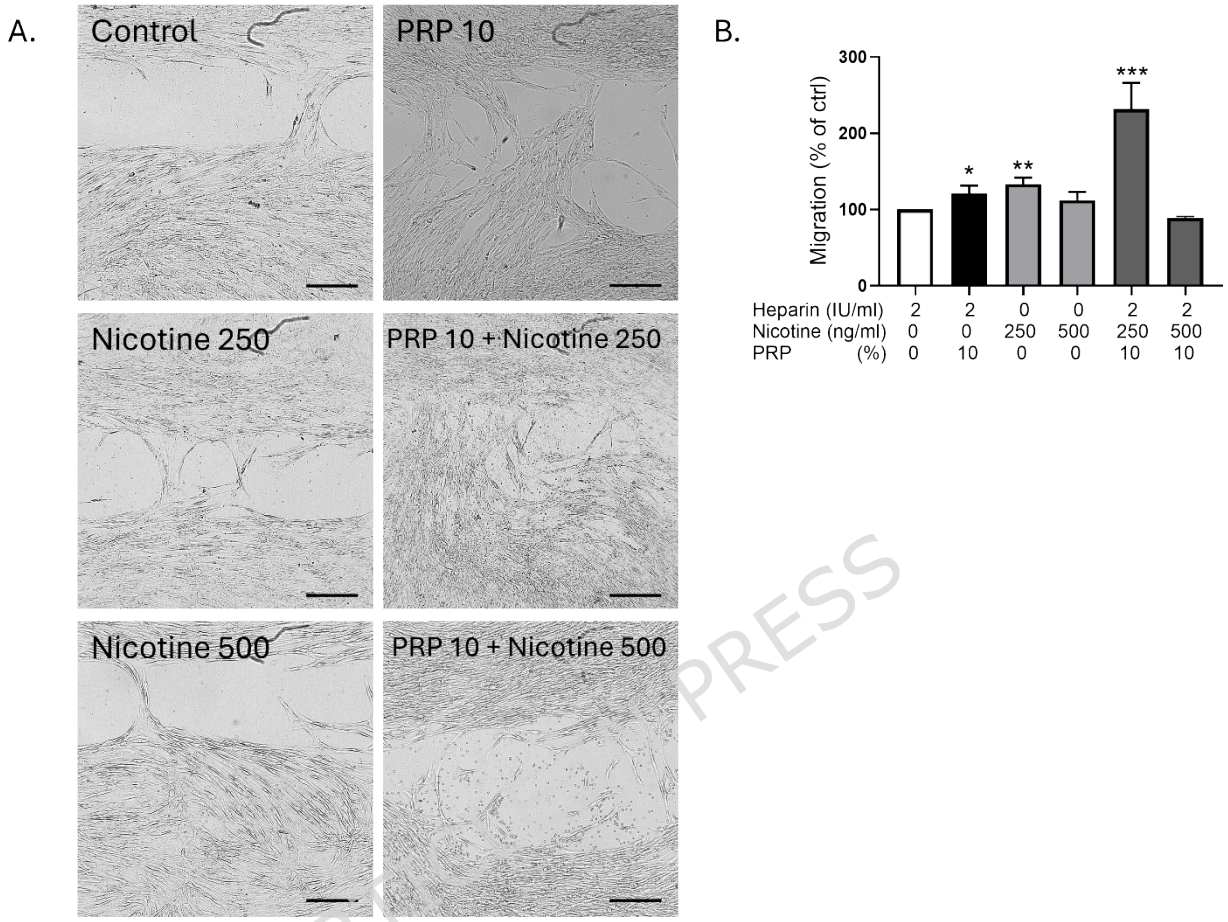

Figure 3. **Effect of nicotine and PRP on the migration of GF.** A. Wound healing pictures of Ibidi chambers after 24 h of GF migration in the presence of the various treatments. B. Wound Healing quantification: areas measured at Day 0 divided by area measured after 24 h of migration. Scale bar= 500 µm. N=8 pictures per experimental condition. *p<0.5, **p < 0.01 and ***p < 0.001. PRP alone and nicotine doses alone were compared to control condition, while the combinations of nicotine and PRP were compared to the nicotine alone respective concentrations.

PRP reduced nicotine-induced cellular senescence in GF.

In vitro senescence was induced by serial passaging of GF at low density from passages 2 to 7, followed by treatment with nicotine and/or PRP. At passage 8, senescence-associated β-galactosidase (SA-β-gal) staining revealed a marked increase in β-gal–positive cells in the nicotine-treated group compared to control, as visualized microscopically (Figure 4A). Quantitative analysis (Figure 4B) showed a non-significant elevation in the proportion of β-gal–positive cells under nicotine exposure. In contrast, PRP treatment significantly reduced the percentage of β-gal-positive cells, both in nicotine-treated and control conditions, demonstrating its anti-senescent effect. The most striking effect was that the 500 ng/ml nicotine induced total cell death that was prevented by

10% PRP addition showing B-gal values even lower than in control condition. These results suggest that PRP mitigates nicotine-induced senescence in GF, supporting its potential regenerative and protective role in maintaining fibroblast function.

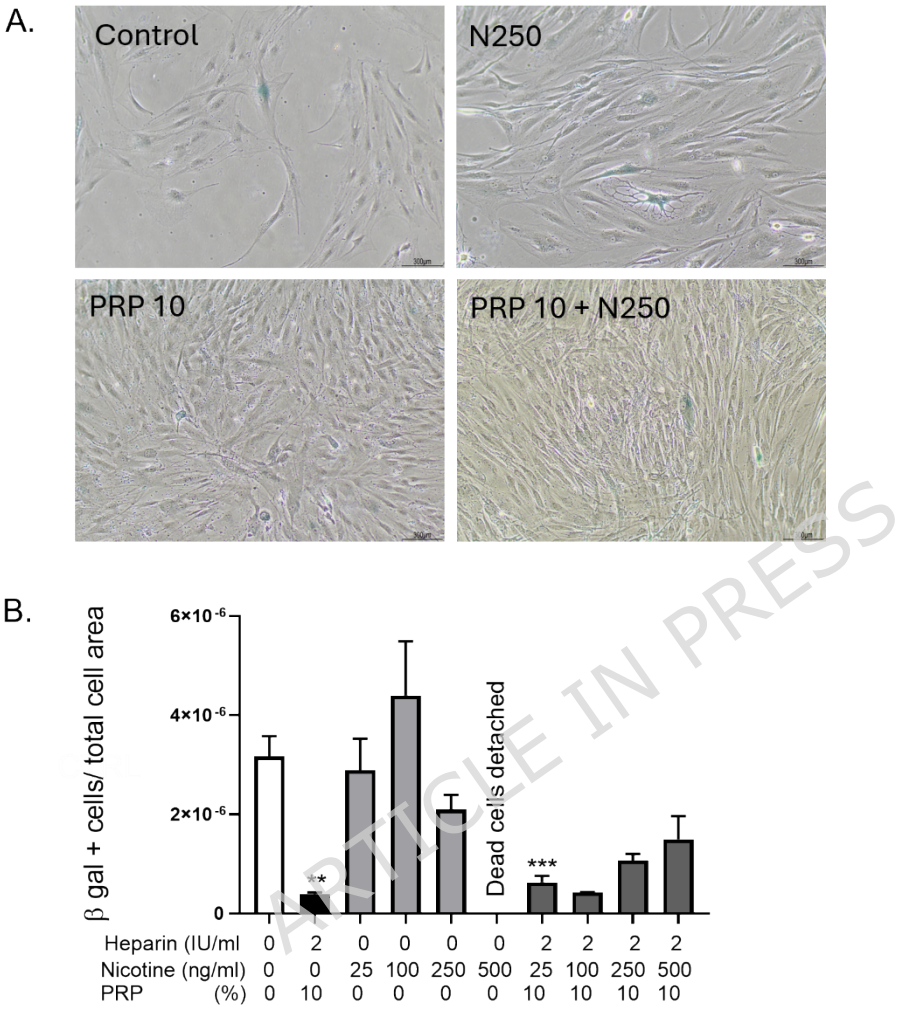

Figure 4: PRP exerted an anti-senescence activity on GF. To evaluate the effect of nicotine and PRP on GF senescence, we induced *in vitro* aging by cultivating the cells at a low density from passages 2 to 6. A. Senescence associated β-galactosidase (SA- beta gal) staining was performed on GF at passage 8 (10x objective lens). B. Quantification of β-gal positive cells reported to the total cell number. *p<0.5, **p < 0.01 and ***p<0.001. n=3 per experimental condition. PRP alone and nicotine doses alone were compared to control condition, while the combinations of nicotine and PRP were compared to the nicotine alone respective concentrations.

Nicotine treatment induced a significant increase in intracellular ROS levels in GF that was neutralized by PRP.

Fluorescence microscopy revealed enhanced green fluorescence intensity in nicotine-treated cells compared to control, indicating elevated ROS production (Figure 5A). Quantitative analysis of

fluorescence per field (Figure 5B) showed a statistically significant increase in ROS levels following nicotine exposure ($p < 0.01$), while co-treatment with PRP markedly reduced ROS accumulation. These findings demonstrate that nicotine promoted oxidative stress in fibroblasts, and that PRP exerted a protective antioxidant effect, attenuating ROS generation.

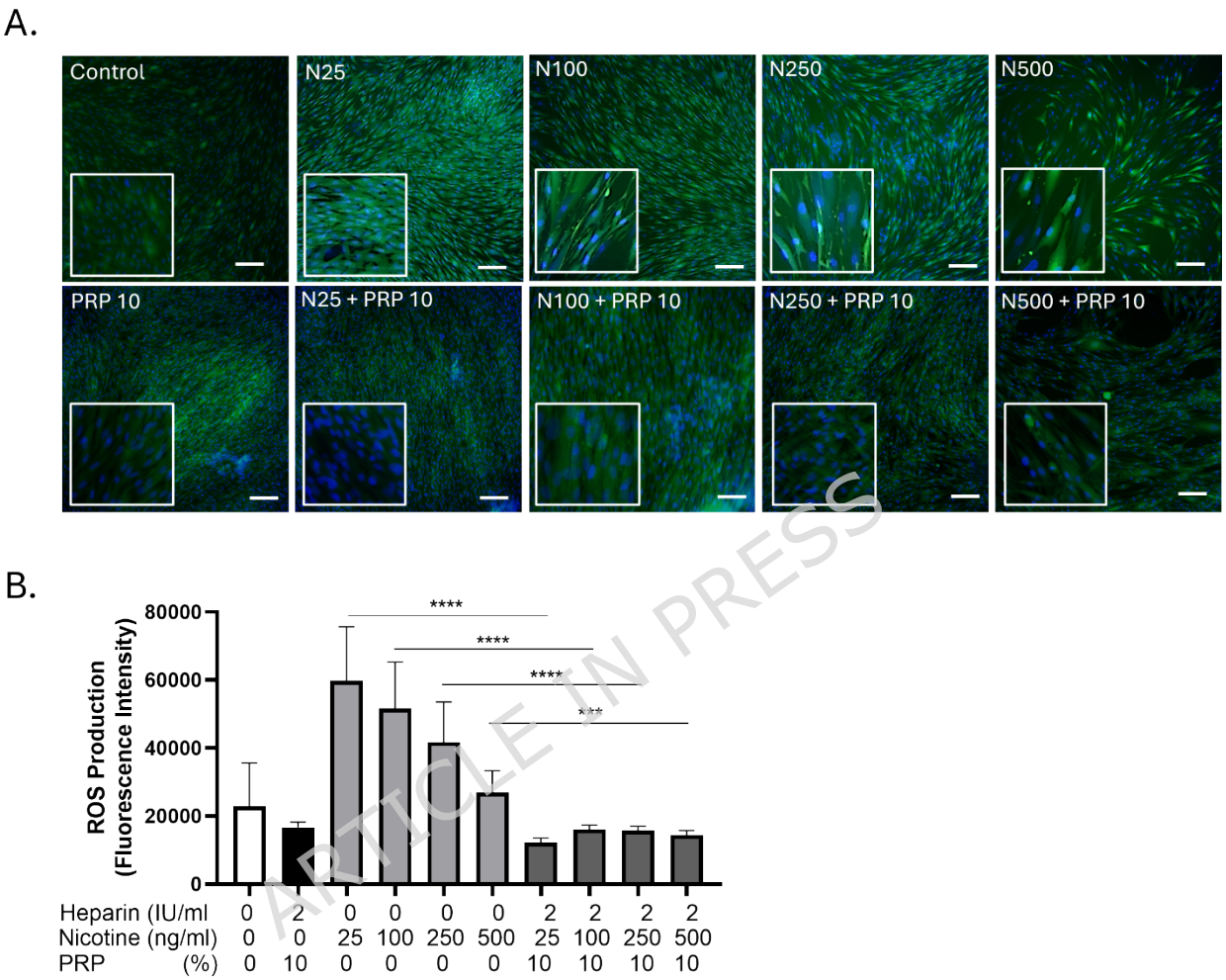

Figure 5: PRP prevented intracellular ROS induced by nicotine in GF. A. Fluorescence imaging: Representative confocal/epifluorescence micrographs of GF after DCF-DA staining (green). Nuclear counterstaining with Hoechst (blue); scale bar = 10 µm. B. Quantification: Average fluorescence intensity per field. Data are expressed as mean ± SEM. Unpaired t test, ***p < 0.001, ****p<0.0001. n=8 per experimental condition. PRP alone and nicotine doses alone were compared to control condition, while the combinations of nicotine and PRP were compared to the nicotine alone respective concentrations.

Nicotine exposure increased the formation of acidic vesicular organelles in GF, an effect that was attenuated by PRP.

After 24 h exposure of GF to nicotine at 250 or 500 ng/mL, acridine orange staining revealed a marked increase in yellow fluorescence, indicating an accumulation of acidic compartments such

as lysosomes or autophagic vacuoles (Figure 6A). An acridine orange signal was spotted at 250 and 500 ng/mL nicotine.

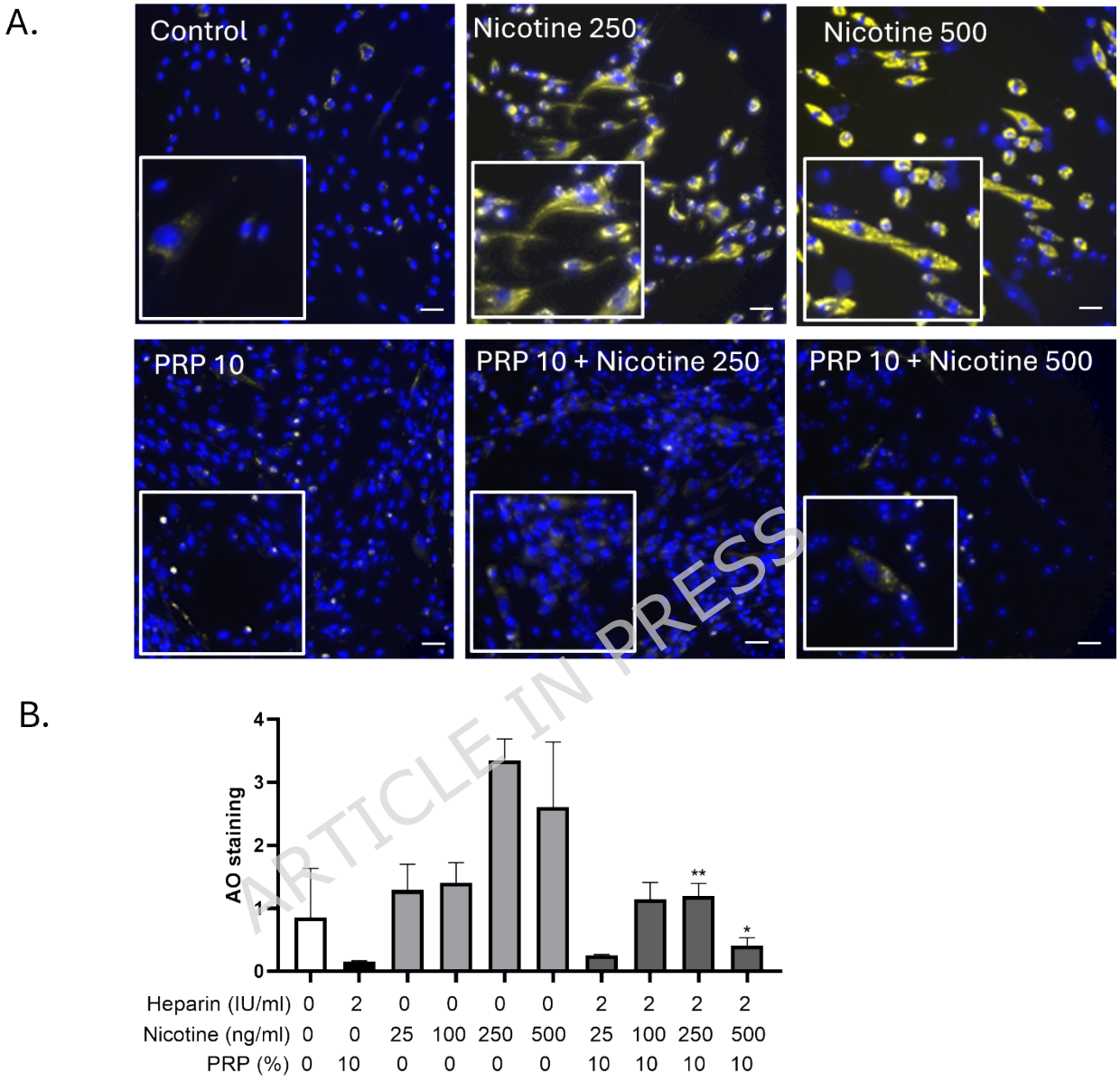

Figure 6: Autophagy evaluation by acridine orange staining of GF following nicotine and/or PRP exposure.

GF were treated with nicotine (250 and 500 ng/ml) and PRP 10% as indicated for 24 h. Acridine orange staining (1 µM , 20 min) was evaluated by fluorescence microscopy, as well as Hoechst nuclear dye (blue) to depict subcellular localization. Scale bar= 50 µm. n=4 per experimental condition. PRP alone and nicotine doses alone were compared to control condition, while the combinations of nicotine and PRP were compared to the nicotine alone respective concentrations.

In contrast, co-treatment with 10% PRP markedly reduced the fluorescence, suggesting a restoration of lysosomal homeostasis and/or reduced autophagic stress. Hoechst nuclear staining

(blue) confirmed proper subcellular localization and overall cell integrity across conditions. These results indicate that nicotine disrupted vesicular acidification in GF, while PRP counteracted these effects, supporting its role in maintaining cellular homeostasis under oxidative or stress-inducing conditions as shown by the quantification (Figure 6B).

PRP conferred significant protective effects against nicotine-induced premature aging in C. elegans.

Lifespan analysis of wild-type N2 worms in liquid culture revealed a reduction in survival along time due to aging, which was partially mitigated by treatment with Plasma-Poor-platelets (blue line, $p < 0.05$), and more robustly by PRP (red line, $p < 0.01$), indicating a dose-dependent protective effect of blood-derived plasma components (Figure 7A). To further assess the impact on cellular aging processes, autophagic flux was evaluated using the mCherry::GFP::LGG-1 reporter strain. Quantification of autolysosomes *via* mCherry fluorescence showed a significant increase in autophagic activity in worms exposed to increasing concentrations of nicotine for 4 days (Figure 7B), reflecting stress-induced autophagy. However, co-treatment with 10% PRP during the final 3 days significantly reduced autolysosome accumulation (Figure 7C and 7D, white bar vs. grey bar), suggesting PRP decreased excessive autophagy linked to nicotine-induced stress. Representative fluorescence images support these findings, displaying visibly reduced mCherry puncta in the PRP-treated group. Collectively, these data indicate that PRP mitigated nicotine-induced lifespan shortening and aberrant autophagic responses in *C. elegans*, underscoring its potential anti-aging and cytoprotective properties.

Profiling of the cytokine secretome by the GF in the presence of increasing concentrations of nicotine, PRP or a combination of both.

To further identify the relevant mediator(s) responsible for cellular deleterious effects of nicotine and the regenerative activity of PRP, a cytokine antibody array was performed (Figure 8). Growth factors released from GF were analyzed, while cultivated with nicotine (25-500 ng/ml), PRP (10%) or a combination of both. The array was performed on the proteins released from GF subjected 3 days to nicotine and then treated for 3 more days in PRP (Figure 8A). Analysis (heat map arrays) of proteins secreted are shown in Figure 8B. A uniform pattern of modulation among the cytokines spotted was observed. An increase of ANG, GRO, Il-6, IL-8, MCP-1, RANTES, TIMP-1 and TIMP-2 in the conditions where PRP is present was depicted, with the most predominant secretion at N25 + PRP 10 for all cytokines. The presence of VEGF-A in the secretome was also observed, however its secretion and modulation were lower than the other cytokines. Examples of four angiogenesis cytokine antibody array membranes for GF cultures with heparin, PRP 10%, Nicotine 500 ng/ml or PRP 10 % and Nicotine 500ng/ml that were used for quantification (Figure 8C).

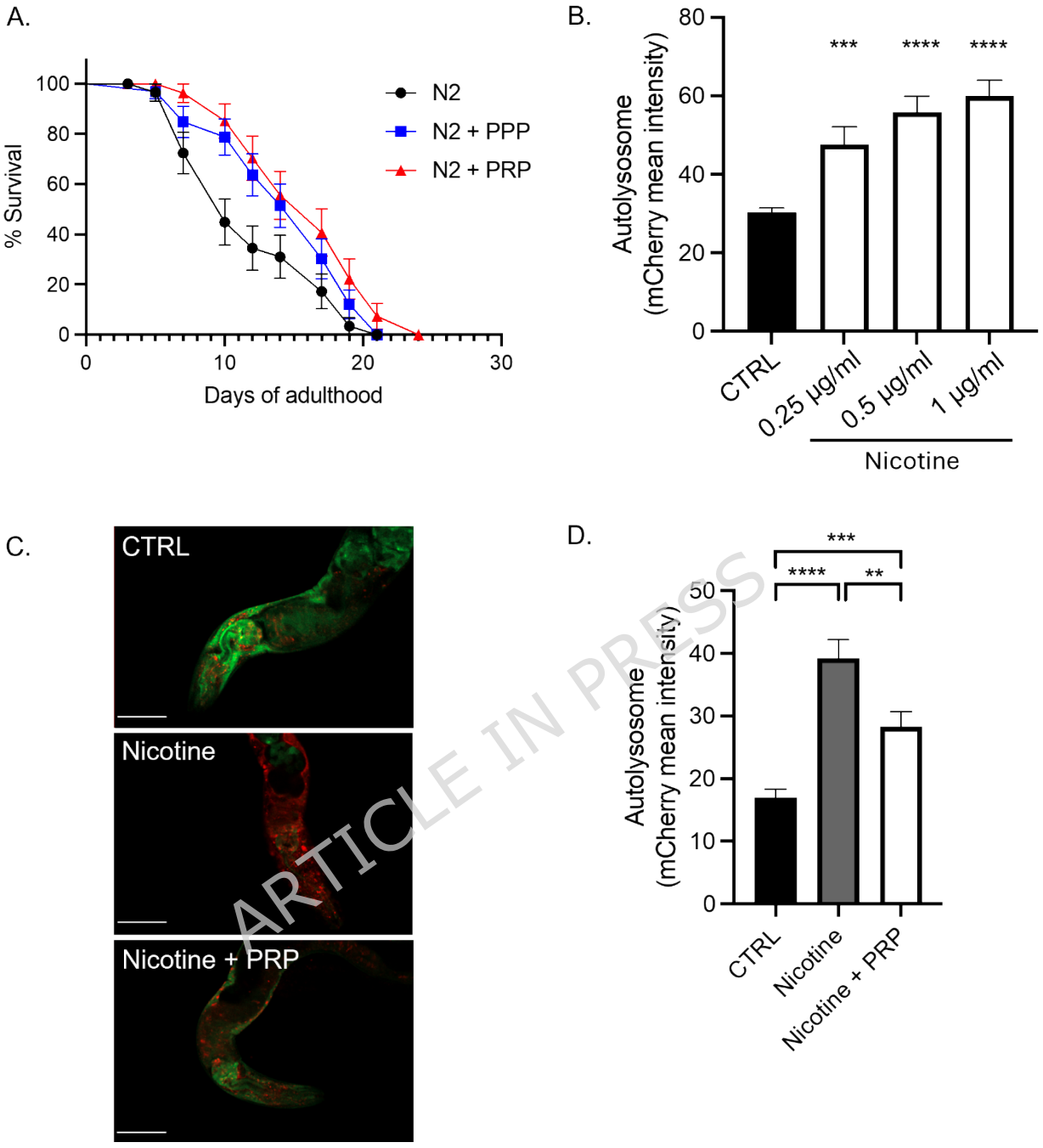

Figure 7: PRP conferred protective effects against nicotine-induced premature aging in *C. elegans.*

A. Lifespan assay on N2 wild type *C. elegans* in liquid culture. PPP (blue line, $p < 0.05$) or PRP (red line, $p< 0.01$) treatment at 10% were compared to the control (black line). B. and C. Autolysosome quantification was realized by measuring mCherry fluorescence from the mCherrry::GFP::LGG-1 strain treated with (B) different concentration of nicotine for 4 days or (C) with 1 µg/ml of nicotine for 4 days (grey bar), in addition to PRP at 10% for the last 3 days (white

bar). One representative image of a *C. elegans* in each condition is depicted, where the scale bar represents 50 µm (C). D. Standard error of mean is represented for each graph. The Log-rank Mantel-cox test was realized for the statistics of the lifespan, and an unpaired t-test was realized for the autolysosome quantification.

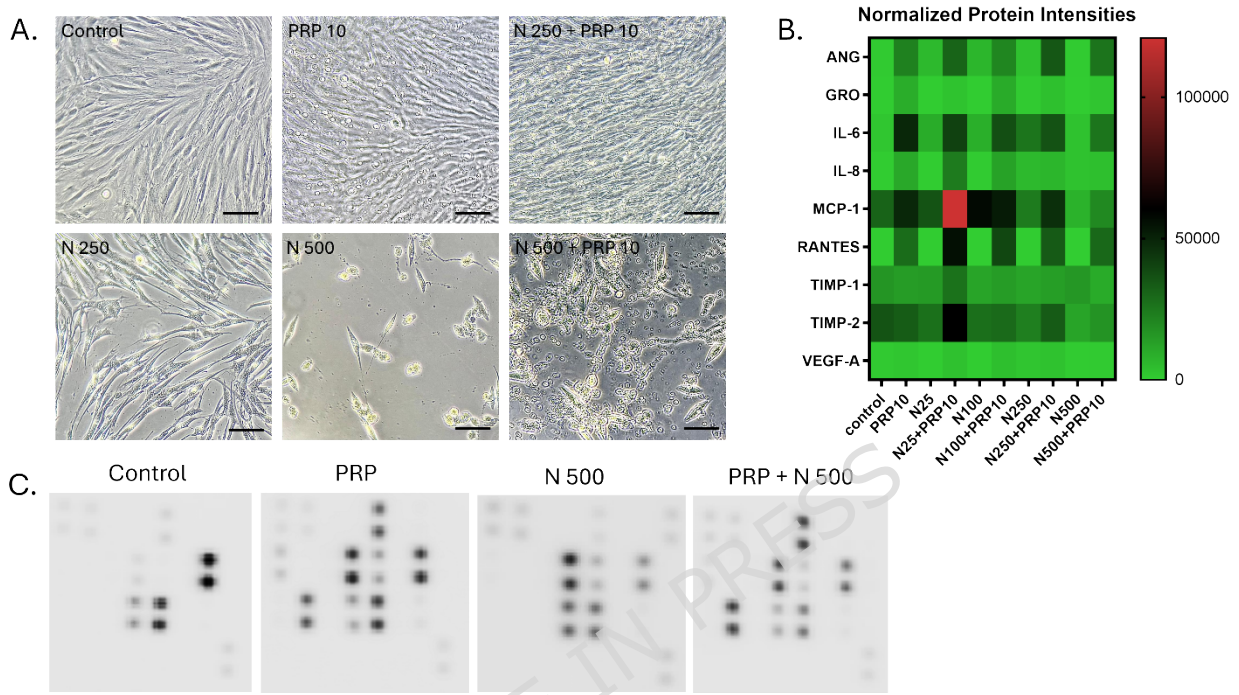

Figure 8: Secretome profiling of cytokines present in the conditioned medium of GF in Nicotine, PRP or both combined.

A. Representative images of the cultures used to produce conditioned medium for secretome profiling on cytokine arrays. Scale bars: 300 µm. B. Heat map analysis representing the average pixel density of the duplicated spots for each cytokine highlighted the array quantified by densitometry. Variation in color intensities represents differential secretion of cytokines by GF, in the presence of PRP, Nicotine (25-500 ng/ml), or the combinations of both. C. Example of the human angiogenesis antibody array composed of duplicated spots of 23 angiogenic and inflammation-related factors performed with the culture supernatants.

Discussion

Gingival fibroblasts (GF) from healthy non-smokers were exposed to nicotine acutely to approximate aspects of the smoker's gingival environment. While this reductionist model is valuable for isolating nicotine-specific cellular responses, it inevitably captures only a limited portion of the biological complexity associated with long-term tobacco use. Chronic smoking involves years of repeated exposure to a diverse mixture of toxicants, oxidants, and inflammatory stimuli that collectively drive persistent alterations in fibroblast function, including epigenetic remodeling, cumulative oxidative damage, dysregulated extracellular matrix turnover, and

impaired wound-healing capacity [16,17]. These long-term adaptations cannot be fully reproduced by short-term nicotine stimulation, which primarily elicits immediate early signaling events rather than the stable phenotypic reprogramming observed *in vivo*. Moreover, fibroblasts in smokers exist within a dynamic microenvironment shaped by interactions with epithelial and immune cells, vascular changes, and smoking-associated shifts in the oral microbiome - factors that are absent in monoculture systems[16]. While the acute nicotine model provides mechanistic insight into early cellular responses, it does not fully recapitulate the chronic pathophysiological state of smoker gingiva, which should be taken into account when interpreting the findings. Further investigations should employ *ex vivo* tissue explants from smokers and non-smokers (e.g., 3D Oral Mucosa Constructs) that are closer to clinical reality than 2D cell culture. Another interesting point would be to treat those constructs with autologous PRP to evaluate eventual systemic alterations in PRP from smokers that would lower its regenerative potential.

In the present study, we aimed to evaluate the effect of PRP on several biological activities of nicotine-treated gingival fibroblasts (GF) and *in vivo* models of *C. elegans*. We hypothesized that PRP could compensate for the negative effects of nicotine on periodontal cells and may therefore be beneficial in the treatment of periodontitis in smokers. Our results showed that PRP modulates several key cellular processes affected by smoking, providing new insight into its potential therapeutic value.

Smoking is a major etiological factor in the development and progression of periodontal diseases and is known to impair the outcomes of periodontal therapy [16,17]. Although nicotine is a major bioactive component of tobacco, it does not account for the full toxicological complexity of cigarette smoke. As highlighted by Holliday *et al.* (2019), nicotine may be unfairly attributed with toxic effects that are primarily driven by other smoke constituents, including reactive aldehydes, polycyclic aromatic hydrocarbons, and particulate matter. Our study therefore examines nicotine-specific effects in isolation, which is relevant in the context of NRT and e-cigarette use, but does not replicate the broader toxicological profile of combustible tobacco. Accordingly, the findings presented here should not be overgeneralized to all forms of tobacco exposure. Future studies incorporating whole cigarette smoke extract or additional smoke-derived toxicants will be necessary to determine whether PRP can mitigate the wider spectrum of smoking-related cellular injury.

GF are among the primary cellular targets of tobacco-related toxicity due to their central role in extracellular matrix production, wound healing, and immune modulation [16]. Nicotine, a key alkaloid in tobacco, disrupts fibroblast functions through oxidative stress, autophagic dysregulation, and pro-inflammatory signaling [18,19]. Our findings confirm and extend prior studies demonstrating that nicotine induces decreased metabolic activity and viability, impaired migration, increased ROS production, elevated lysosomal activity, morphological changes, and premature cellular senescence—each of which contributes to impaired periodontal healing [20].

Previous literature has described biphasic effects of nicotine, with low concentrations promoting proliferation in mesenchymal stem cells [21], whereas higher concentrations are cytotoxic, inhibiting proliferation, protein synthesis, and attachment [22]. In our study, clinically relevant nicotine concentrations (50–500 ng/mL; ≈0.3–3.0 μM) were chosen to reflect systemic exposure levels in smokers [23,24].

In contrast, our study did not observe proliferative enhancement at low nicotine concentrations in GF. This discrepancy likely reflects intrinsic differences between stem cells and differentiated fibroblasts, including proliferative capacity, receptor expression, and sensitivity to oxidative stress. Differences in exposure duration, serum conditions, and nicotine delivery methods across studies may also contribute to divergent outcomes. High nicotine concentrations have been shown to inhibit collagen and fibronectin synthesis [25], reduce alkaline phosphatase activity [25], and stimulate ROS generation leading to mitochondrial damage [26]. The significant increase in intracellular ROS observed in our nicotine-treated GF supports nicotine's role as a potent oxidative stressor. Similarly, the increase in acidic vesicular organelles, indicating autophagic activity, aligns with previous observations in cardiomyocytes [27]. Nicotine has also been reported to destabilize lysosomes, possibly through oxidative mechanisms [28]. Furthermore, our study confirmed nicotine-induced senescence in GF via β-gal staining, consistent with reports of accelerated aging in lung and skin fibroblasts exposed to tobacco constituents [29]. Variability in the magnitude of senescence reported across studies may reflect differences in nicotine concentration, exposure duration, or donor-specific fibroblast characteristics.

Platelet-Rich Plasma (PRP), a preparation containing concentrated platelets suspended in plasma, has shown increasing promise in tissue engineering and regenerative medicine due to its rich content of growth factors such as PDGF, VEGF, and TGF-β [30,31]. In our study, 10% PRP supplementation significantly increased cell proliferation and restored metabolic activity, improved migration, and mitigated ROS generation, lysosomal stress, and cellular senescence in nicotine-exposed GF. These findings are consistent with previous reports showing that PRP enhances fibroblast proliferation, collagen synthesis, and extracellular matrix remodeling [32]. However, our results extend prior work by demonstrating that PRP also restores autophagic flux, suggesting a broader cytoprotective mechanism. TGF-β and PDGF are known to modulate mTOR and SMAD signaling cascades, both of which intersect with autophagy regulation and have homologs in *C. elegans* [33,34]. Other studies have shown that PRP reduces IL-6 and TNF-α levels, likely through inhibition of NF-κB signaling [35], supporting its anti-inflammatory potential.

Cytokine profiling of the secretome of nicotine-exposed GF revealed increased levels of MCP-1, IL-6, RANTES/CCL5, and TIMP-2 following PRP treatment. These cytokines have previously been associated with autophagy-related pathways, suggesting a potential link between inflammatory signaling and autophagic regulation. TIMP-2, a known inhibitor of MMPs, regulates extracellular matrix degradation and angiogenesis. In pancreatic stellate cells, autophagy inhibition has been associated with reduced TIMP-2 and increased MMPs [36], indicating a relationship

between autophagy and extracellular matrix regulation. MCP-1, a key chemokine involved in immune cell recruitment, has been linked to autophagy-related processes [37,38], and the autophagy adaptor protein p62 has been shown to regulate MCP-1 expression [39]. Enhanced autophagic activity has also been associated with increased MCP-1 and IL-6 in synovial fluid neutrophils [40]. IL-6 activates the JAK/STAT3 pathway and has been reported to modulate autophagy in a context-dependent manner, often inhibiting it [41]. Similarly, RANTES/CCL5 activates mTOR signaling and has been associated with autophagy inhibition [42,43]. Together, these observations suggest that the increased cytokine levels observed following nicotine and PRP exposure may be associated with modulation of autophagic responses. It is plausible that RANTES/CCL5 and IL-6 are overexpressed after nicotine + PRP treatment to dampen autophagy and prevent excessive activation. However, this hypothesis requires further mechanistic validation.

The autophagy process is crucial for survival across species and becomes less effective with aging, particularly in *C. elegans*. This model is especially valuable for investigating age-dependent changes in autophagic responses that cannot be adequately captured in cell culture systems. For this reason, our study was conducted using age-synchronized young nematodes. The transparency of the nematode allows *in vivo* tracking and quantification of autophagic processes across different organs using the mCherry::GFP::LGG-1 reporter. Our data suggest that PRP exerts anti-senescent activity, a mechanism previously underexplored in periodontal research. In *C. elegans*, nicotine induced hyperactivation of autophagy, resembling an accelerated aging phenotype [44]. PRP exposure reduced autolysosomal accumulation and improved survival under nicotine-induced stress, supporting the evolutionary conservation of its cytoprotective effects. However, the human periodontal microenvironment differs substantially from that of the nematode, and PRP's anti-autophagic and anti-senescent effects in humans remain to be validated in more physiologically relevant models.

These findings have significant relevance for periodontal therapy in smokers. Nicotine-induced impairment in GF function contributes to delayed healing, reduced tissue regeneration, and greater susceptibility to chronic periodontitis [19,45,46]. PRP's ability to counteract these effects makes it a compelling adjunct in regenerative dentistry, particularly for patients with tobacco exposure. A recent systematic review underscored the potential of PRP as a valuable adjunct in oral surgery, demonstrating significant benefits in soft-tissue regeneration and, to a lesser extent, hard-tissue regeneration, with no distinction between smokers and non-smokers [47].However, translation to clinical practice warrants caution. Our study was limited to in vitro experiments using primary fibroblasts from non-smokers and invertebrate models. Gingival fibroblasts from healthy non-smokers were exposed to nicotine acutely to approximate aspects of the smoker's gingival environment. While this reductionist model is valuable for isolating nicotine-specific cellular responses, it inevitably captures only a limited portion of the biological complexity associated with long-term tobacco use. Chronic smoking involves years of repeated exposure to a diverse mixture of toxicants, oxidants, and inflammatory stimuli that collectively drive persistent alterations in fibroblast function, including epigenetic remodeling, cumulative oxidative damage, dysregulated

extracellular matrix turnover, and impaired wound-healing capacity. These long-term adaptations cannot be fully reproduced by short-term nicotine stimulation, which primarily elicits immediate early signaling events rather than stable phenotypic reprogramming. Moreover, fibroblasts in smokers exist within a dynamic microenvironment shaped by interactions with epithelial and immune cells, vascular changes, and smoking-associated shifts in the oral microbiome - factors absent in monoculture systems. Therefore, while the acute nicotine model provides important mechanistic insight, its limitations in recapitulating the chronic pathophysiological state of smoker gingiva should be acknowledged. Future investigations should employ *ex vivo* tissue explants from smokers and non-smokers (e.g., 3D oral mucosa constructs) that more closely reflect clinical reality than 2D cell culture. Another important direction would be to treat these constructs with autologous PRP to evaluate whether systemic alterations in smokers affect PRP composition and reduce its regenerative potential.

It is important to emphasize that, despite the cytoprotective and pro-regenerative effects observed in our experimental models, these findings should not be interpreted as suggesting that PRP can compensate for the well-documented clinical consequences of tobacco use. Smoking cessation remains the most effective and evidence-based intervention for improving periodontal health in smokers, and no adjunctive therapy - including PRP - can replicate the broad systemic and local benefits associated with quitting smoking. Accordingly, PRP should be viewed as a potential supportive strategy aimed at mitigating some of the cellular dysfunctions induced by nicotine exposure, rather than as an alternative to cessation. The therapeutic relevance of PRP in smokers must therefore be interpreted within this context and validated in clinical studies specifically designed to evaluate outcomes in individuals who continue to smoke.

From a clinical standpoint, the cytoprotective and pro□regenerative effects observed in our experimental models suggest that PRP may hold promise as an adjunctive strategy for managing periodontitis in patients who continue to smoke. Smoking is well known to impair wound healing, reduce fibroblast proliferation, increase oxidative stress, and compromise regenerative outcomes, and the ability of PRP to enhance cell viability, migration, and stress resistance may help counteract some of these detrimental effects. PRP could therefore be beneficial in procedures requiring soft□tissue healing or regenerative support, such as periodontal surgery, intrabony defect treatment, or soft□tissue augmentation, where smokers typically exhibit delayed or suboptimal responses. However, these potential advantages must be interpreted with caution, as PRP cannot overcome the systemic and local biological consequences of ongoing tobacco exposure, and smoking cessation remains the most effective and evidence□based intervention for improving periodontal outcomes. The clinical relevance of PRP in smokers thus remains hypothetical at this stage and requires validation through well□designed clinical trials specifically assessing whether PRP can meaningfully enhance periodontal healing in individuals who continue to smoke.

Materials and methods

Human subjects

This study was conducted in accordance with the principles outlined in the Declaration of Helsinki. Ethical approval was obtained from the Ethics Committee CCER Geneva ethics committee (ID 2017–00700, approved on 18th October 2018, and informed consent was obtained from all participants prior to enrollment. Human GF were obtained from biopsies of donors clinically treated for various reasons.

All experiments were performed in accordance with relevant guidelines and regulations.

PRP was prepared from the blood retrieved from healthy volunteers under the same ethical authorization.

Cell cultures

After washing with Dulbecco's Phosphate Buffered Saline solution (DPBS, Gibco) to dilute the oral bacterial flora of the gingival tissue, small fragments of biopsy (2 mm square) were plated in culture dishes in control growth medium (GM): DMEM (Capricorn Scientific) containing 10% heat-inactivated fetal bovine serum (FBS, Capricorn Scientific) and 1% penicillin-streptomycin (Pan Biotech). Dishes were incubated at 37°C in 5% CO_2 humidified atmosphere for 48 h, undisturbed. After 48 h, the medium was replaced. Two different donors were used to conduct all the experiments. The procedure conformed to the principles of the Declaration of Helsinki and was approved by CCER Geneva ethics committee (ID 2017–00700, approved on 18th October 2018). GF were used between passages 2 to 10.

Preparation of human allogenic PRP and PPP

Allogenic blood samples from donors were processed into specific medical devices (RegenKit-BCT, Regen Lab SA) following a precise standardized protocol [48]. These devices produce a standardized leucocyte poor PRP thanks to a separator gel that isolates the plasma and the platelets from the other blood components. Ten ml of blood were collected per tube and centrifuged at room temperature for 5 min in a Regen Lab centrifuge (Drucker Horizon-6-FA) at a force of 1500 x g. Subsequently, the red and white blood cells are stacked at the bottom of the tube under the separator gel, whereas the platelets were sedimented above the gel layer with the plasma floating above them. After a resuspension step, around 5.5 mL PRP per tube were obtained and stored until use for a maximum of 15 days at room temperature in a polypropylene tube (Becton-Dickinson). To obtain platelet-poor plasma (PPP), we collected the plasma directly after centrifugation without the resuspension step.

Platelets, red and white blood cells, as well as mean platelet volume were counted (Sysmex) in whole blood before centrifugation and in the prepared PRP/PPP before addition to culture media. In all PRP/PPP conditions, heparin (Leo) was added (2UI/ml) to prevent clot formation.

The hematological characteristics of PRP obtained with this device have been extensively validated by Gomri et al. (Pharmaceutics, 2021), who demonstrated that RegenKit-BCT consistently

produces a pure platelet-rich plasma (P-PRP) with a 1.6- to 1.8-fold increase in platelet concentration relative to baseline whole blood, while achieving >99% depletion of red blood cells and very low leukocyte content. Importantly, the mean platelet volume (MPV) remains unchanged compared to whole blood, indicating preservation of platelet morphology and activation state. As our PRP preparations were generated using the same closed, gel-separator system and protocol, their composition falls within the validated ranges as previously reported [48].

Cell proliferation assays

GF proliferation was measured by using a ready-to-use solution containing stable tetrazolium salt WST-1 (Cell Proliferation Reagent WST-1, Sigma-Aldrich). Ninety-six well plates were seeded with 5 x 10^3 cells and incubated for 2 hours in GM at 37°C in 5% CO2 humidified atmosphere. GM with nicotine ((-)-Nicotine, Sigma-Aldrich) at different final concentrations (25 ng/ml, 100 ng/ml, 250 ng/ml, 500 ng/ml) was added to each well. The medium was replaced after 48 h and complemented with 10% PRP. After 2 and 5 days of incubation, 10 µl of Cell Proliferation Reagent WST-1 were added to each well and the plate was incubated for 4 h before the measure of the absorbance of the formazan at 460 nm in a Cytation plate reader (Biotek).

Crystal violet viability assay

GF were plated at a density of 5 x10^3 cells per well in 96-well plates. Cells were treated with various final concentrations of nicotine (25, 100, 250 and 500 ng/ml) in GM. After 48 h, the medium was replaced and complemented with 10% PRP. After 2 and 5 days of incubation, cells were fixed with 100 µl of methanol at -20°C for 15 min. A solution of 0.1% crystal violet (100 µl) was added to each well for 10-15 min, washed with distilled water and air-dried. Cytation reader was used to image the plates. Samples were then dissolved with glacial acetic acid, and the optical density at 570 nm was determined using an automatic microplate reader (Biotek).

CellTiter-Glo ® luminescent Cell cell viability assay

GF were plated in GM at a density of 5 x10^3 cells per well in 96-well plates for 2 hours to allow cell attachment. Culture media with nicotine [25-500 ng/ml] was used for 6 days, and 10 % PRP-was added to the nicotine culture media for 3 more days. Cell viability was assessed in accordance with the manufacturer's instructions. Luminescence was recorded on a Cytation multi-mode reader in relative light units (RLU).

Live/Dead test

GF were seeded at a density of 5 x 10^3 cells in 96-well plates and incubated for 2 h at 37°C in 5% CO_2 humidified atmosphere. DMEM with nicotine ((-)-Nicotine, Sigma-Aldrich) at different final concentrations (25 ng/ml, 100 ng/ml, 250 ng/ml, 500 ng/ml) was added to each well. After 48 h, 10% PRP were added to the different conditions. At the end of 2 days of incubation, Live/Dead assay (Invitrogen) was performed following standard protocol of manufacturer to determine

viability of GF cells. The discrimination of live cells from dead cells was realized by respectively and simultaneously staining with green fluorescent calcein to indicate esterase activity and red-fluorescent ethidium bromide to indicate loss of plasma membrane integrity by visualization on Cytation. Gen 5 software was used to quantify the amount of calcein positive cells in the wells.

Wound migration assay

GF at a density of 4×10^5/ml (70 µl volume) were added to 24-well plates with culture insert (Ibidi). The cells were incubated at 37 °C for 24 h to allow cell attachment. Then, a cell-free gap of 500 µm was created by removal of the culture insert. For the measurement of cell migration, 250 µL of mitomycin C (Thermo Fisher Scientifics) at 0.4 mg/ml was added to each well to avoid cell proliferation. Medium was replaced by test media in triplicates: DMEM, heparin (2 IU/ml) supplemented with 10 % FBS, 10 % PRP, nicotine 250 ng/ml, nicotine 500 ng/ml alone or combined with 10% PRP. Images were captured after 24 h using an inverted phase-contrast microscope at 4× magnification. The percentage of wound closure was calculated with ImageJ software.

Chronicity and senescence test

GF cells were seeded at low densities (2×10^3) in 35 mm Petri dishes (Falcon) and incubated for 2 h at 37°C in a 5 % CO2 humidified atmosphere. DMEM with nicotine ((-)-Nicotine, Sigma-Aldrich) at different final concentrations (25, 100, 250 and 500 ng/ml) was added to each well. When the cells were confluent, they were passed to other 35 mm Petri dishes using TrypLE (Gibco). This procedure was repeated weekly over a period of one month until P10. Cell seeding concentrations decreased over time due to cell damage with 250 and 500 ng/ml nicotine experimental conditions. GF cells were fixed and stained following the protocol of senescence associated (SA) β-Galactosidase Staining kit (Cell Signaling Technology), designed to detect β-galactosidase activity, a known characteristic of senescent cells. Quantification was made with ImageJ software by measuring the total cell surface and counting the SA-β-galactosidase positive cells.

DCFDA cellular ROS assay

Intracellular reactive oxygen species (ROS) was assessed using the DCFDA Cellular ROS Detection Assay Kit (Abcam), according to the manufacturer's protocol and as previously described [49]. GF were cultured in 96 well plates (1×10^4 cells/well) for 48 h with increasing concentrations of nicotine (50-500 ng/ml) and then 10% PRP was added for 3 days. The concentrations of the positive control [tert-butyl hydroperoxide (TBHP)] was 200 µmol/l. Fluorescence at 483-14 nm/530-30 nm was recorded from 3 h up to 24 h post-treatment, using the Cytation microplate reader. Background fluorescence was subtracted from each value before fold increase in fluorescence intensity relative to the negative control (GM) was determined.

Acridine orange staining

Cells were seeded in 24-well microclear optical plates (1 x 10^4 cells/well). After 24h, they were incubated with increasing concentrations of nicotine for 48 h, followed by 10% PRP addition for 3 more days. Then, the cells were stained with medium containing 1 µg/ml acridine orange for 15 min at 37 °C, washed twice in PBS and immediately observed with a Cytation imager. The cytoplasm and nucleus of acridine orange-stained cells fluoresced bright green, whereas the acidic autophagic vacuoles fluoresced bright red, as described previously [50,51].

***C. elegans* strains and maintenance**

Standard methods for culturing and handling *C. elegans* were followed [14]. *C. elegans* was maintained on standard nematode growth medium (NGM) plates streaked with OP50 *E. coli*. The strains used in this study were obtained from the *C. elegans* Genetics Center (University of Minnesota, MN, USA). Animals were transferred to fresh NGM plates without floxuridine (FUdR) every 2 days to ensure maintenance. The strains used in this study include the N2 Bristol strain and MAH215 sqIs11[lgg-1p::mCherry::GFP::lgg-1 + rol-6].

Lifespan in N2 wild-type *C. elegans* with PRP and PPP

Animals at larval stage 4 (L4) were divided into triplicates in a 96-well plate, with 10 worms per well in 150 µL of liquid culture medium (S Basal, 10 mM potassium citrate pH 6, 10 mM metal solution, 30 mM CaCl□, 30 mM MgSO□, 50 µM FuDR) supplemented with OP50 [52] Freshly prepared platelet-poor plasma (PPP) or PRP was added at 10% of the total volume in designated wells, along with heparin (2UI/ml) [53].The animals were counted every other day, and the medium was refreshed every 2 days. Experiment was done three independent times. Graphs were generated using GraphPad Prism 9.

Confocal microscopy in MAH215 sqIs11 *C. elegans*

L4 *C. elegans* were synchronized [14] and deposited (10 worms) in 150 µL of liquid culture medium (S Basal, 10 mM potassium citrate pH 6, 10 mM metal solution, 30 mM CaCl□, 30 mM MgSO□, 50 µM FuDR) with OP50 *E. coli* bacteria in a 96-well plate [52]. Nicotine titration was performed over 4 days by adding 10 ng/mL, 100 ng/mL, or 1 µg/mL of nicotine to the liquid culture. To assess the effect of PRP on autophagy, 10% freshly prepared PPP or PRP was added to the culture medium, along with heparin (2UI/ml). Before imaging, worms were placed on a drop of 60% glycerol on a 2% agarose pad and imaged using a Zeiss LSM800 confocal microscope. Autolysosomes quantifications were performed in the anterior part of the intestine, where autophagy is most prominent, using QuPath software. The mean fluorescence intensity of the selected area is represented. Experiment was done three independent time.

Angiogenesis Protein Array in GF

RayBio Human Angiogenesis Antibody Arrays C-1000 (RayBiotech) were used to assay the GF-secreted cytokines in conditioned medium containing 10% PRP, Nicotine (25-100-250-500 ng/ml) or a combination of both. To prepare the conditioned medium, GF were seeded in T25 flasks at a concentration of 5×10^5 cells per flask in complete growth medium. The following day, the medium

was replaced with DMEM and 0.5% FBS, and the cells were treated with the different experimental conditions After 48 h, the medium was collected and centrifuged at 400× g for 5 min to remove cellular debris. The membranes were incubated with fresh supernatants. In the array, 30 angiogenic cytokines, chemokines, enzymes and growth factors were measured according to the manufacturer's protocol. Membranes were imaged using a Fusion System (Vilber Lourmat). Protein levels were quantified using the Protein Array Analyzer in the ImageJ program. Values were normalized to reference spots on the membranes.

Statistics

Data are presented as mean ± SD, and statistical differences were determined using the statistical test specified in the figure legends, with * $p < 0.05$, ** $p < 0.01$, ***$p < 0.001$, and **** $p < 0.0001$. For the comparison of two populations, a t-test or Mann–Whitney test was used depending on the normality of the dataset. For the comparison of more than two populations, either ANOVA or the Kruskal–Wallis test was used, depending on the normality of the dataset. For each cell culture experiment, treatments were performed minimum in triplicate, quadruplicate or 8 replicates. Unless otherwise stated, each experiment was repeated three times.

References

1 Kinane, D. F., Stathopoulou, P. G. & Papapanou, P. N. Periodontal diseases. *Nature reviews. Disease primers* **3**, 17038 (2017). https://doi.org/10.1038/nrdp.2017.38

2 Kinane, D. F. Causation and pathogenesis of periodontal disease. *Periodontology 2000* **25**, 8-20 (2001). https://doi.org/10.1034/j.1600-0757.2001.22250102.x

3 Giannopoulou, C., Geinoz, A. & Cimasoni, G. Effects of nicotine on periodontal ligament fibroblasts in vitro. *Journal of clinical periodontology* **26**, 49-55 (1999). https://doi.org/10.1034/j.1600-051x.1999.260109.x

4 Kang, S. W. *et al.* Effects of nicotine on apoptosis in human gingival fibroblasts. *Archives of oral biology* **56**, 1091-1097 (2011). https://doi.org/10.1016/j.archoralbio.2011.03.016

5 Pabst, M. J. *et al.* Inhibition of neutrophil and monocyte defensive functions by nicotine. *Journal of periodontology* **66**, 1047-1055 (1995). https://doi.org/10.1902/jop.1995.66.12.1047

6 Holliday, R. S., Campbell, J. & Preshaw, P. M. Effect of nicotine on human gingival, periodontal ligament and oral epithelial cells. A systematic review of the literature. *J Dent* **86**, 81-88 (2019). https://doi.org/10.1016/j.jdent.2019.05.030

7 Apatzidou, D. A. The role of cigarette smoking in periodontal disease and treatment outcomes of dental implant therapy. *Periodontology 2000* **90**, 45-61 (2022). https://doi.org/10.1111/prd.12449

8 Gomez-Virgilio, L. *et al.* Autophagy: A Key Regulator of Homeostasis and Disease: An Overview of Molecular Mechanisms and Modulators. *Cells* **11** (2022). https://doi.org/10.3390/cells11152262

9 Zhang, W. *et al.* Platelet-Rich Plasma for the Treatment of Tissue Infection: Preparation and Clinical Evaluation. *Tissue engineering. Part B, Reviews* **25**, 225-236 (2019). https://doi.org/10.1089/ten.TEB.2018.0309

10 Arpornmaeklong, P., Kochel, M., Depprich, R., Kubler, N. R. & Wurzler, K. K. Influence of platelet-rich plasma (PRP) on osteogenic differentiation of rat bone marrow stromal cells. An in vitro study. *International journal of oral and maxillofacial surgery* **33**, 60-70 (2004). https://doi.org/10.1054/ijom.2003.0492

11 Berndt, S., Turzi, A., Pittet-Cuenod, B. & Modarressi, A. Autologous Platelet-Rich Plasma (CuteCell PRP) Safely Boosts In Vitro Human Fibroblast Expansion. *Tissue engineering. Part A* **25**, 1550-1563 (2019). https://doi.org/10.1089/ten.TEA.2018.0335

12 Kobayashi, E. *et al.* Effects of platelet rich plasma (PRP) on human gingival fibroblast, osteoblast and periodontal ligament cell behaviour. *BMC oral health* **17**, 91 (2017). https://doi.org/10.1186/s12903-017-0381-6

13 Wang, X., Zhang, Y., Choukroun, J., Ghanaati, S. & Miron, R. J. Effects of an injectable platelet-rich fibrin on osteoblast behavior and bone tissue formation in comparison to platelet-rich plasma. *Platelets* **29**, 48-55 (2018). https://doi.org/10.1080/09537104.2017.1293807

14 Xu, J., Gou, L., Zhang, P., Li, H. & Qiu, S. Platelet-rich plasma and regenerative dentistry. *Aust Dent J* **65**, 131-142 (2020). https://doi.org/10.1111/adj.12754

15 Sun, J. *et al.* Emerging roles of platelet concentrates and platelet-derived extracellular vesicles in regenerative periodontology and implant dentistry. *APL bioengineering* **6**, 031503 (2022). https://doi.org/10.1063/5.0099872

16 Heasman, L. *et al.* The effect of smoking on periodontal treatment response: a review of clinical evidence. *Journal of clinical periodontology* **33**, 241-253 (2006). https://doi.org/10.1111/j.1600-051X.2006.00902.x

17 Kinane, D. F. & Chestnutt, I. G. Smoking and periodontal disease. *Crit Rev Oral Biol Med* **11**, 356-365 (2000). https://doi.org/10.1177/10454411000110030501

18 Raulin, L. A., McPherson, J. C., 3rd, McQuade, M. J. & Hanson, B. S. The effect of nicotine on the attachment of human fibroblasts to glass and human root surfaces in vitro. *Journal of periodontology* **59**, 318-325 (1988). https://doi.org/10.1902/jop.1988.59.5.318

19 Tipton, D. A. & Dabbous, M. K. Effects of nicotine on proliferation and extracellular matrix production of human gingival fibroblasts in vitro. *Journal of periodontology* **66**, 1056-1064 (1995). https://doi.org/10.1902/jop.1995.66.12.1056

20 Colombo, G. *et al.* Oxidative damage in human gingival fibroblasts exposed to cigarette smoke. *Free Radic Biol Med* **52**, 1584-1596 (2012). https://doi.org/10.1016/j.freeradbiomed.2012.02.030

21 Kim, B. S. *et al.* Effects of nicotine on proliferation and osteoblast differentiation in human alveolar bone marrow-derived mesenchymal stem cells. *Life Sci* **90**, 109-115 (2012). https://doi.org/10.1016/j.lfs.2011.10.019

22 Chioran, D. *et al.* Nicotine Exerts Cytotoxic Effects in a Panel of Healthy Cell Lines and Strong Irritating Potential on Blood Vessels. *Int J Environ Res Public Health* **19** (2022). https://doi.org/10.3390/ijerph19148881

23 Benowitz, N. L., Bernert, J. T., Caraballo, R. S., Holiday, D. B. & Wang, J. Optimal serum cotinine levels for distinguishing cigarette smokers and nonsmokers within different racial/ethnic groups in the United States between 1999 and 2004. *Am J Epidemiol* **169**, 236-248 (2009). https://doi.org/10.1093/aje/kwn301

24 Benowitz, N. L., Hukkanen, J. & Jacob, P., 3rd. Nicotine chemistry, metabolism, kinetics and biomarkers. *Handb Exp Pharmacol*, 29-60 (2009). https://doi.org/10.1007/978-3-540-69248-5_2

25 Marinucci, L., Bodo, M., Balloni, S., Locci, P. & Baroni, T. Sub-toxic nicotine concentrations affect extracellular matrix and growth factor signaling gene expressions in human osteoblasts. *J Cell Physiol* **229**, 2038-2048 (2014). https://doi.org/10.1002/jcp.24661

26 Caliri, A. W., Tommasi, S. & Besaratinia, A. Relationships among smoking, oxidative stress, inflammation, macromolecular damage, and cancer. *Mutat Res Rev Mutat Res* **787**, 108365 (2021). https://doi.org/10.1016/j.mrrev.2021.108365

27 Xing, R. *et al.* Low-dose nicotine promotes autophagy of cardiomyocytes by upregulating HO-1 expression. *Biochem Biophys Res Commun* **522**, 1015-1021 (2020). https://doi.org/10.1016/j.bbrc.2019.11.086

28 Wu, X. *et al.* Dual Regulation of Nicotine on NLRP3 Inflammasome in Macrophages with the Involvement of Lysosomal Destabilization, ROS and alpha7nAChR. *Inflammation* **48**, 61-74 (2025). https://doi.org/10.1007/s10753-024-02036-z

29 Rinaldi, S. *et al.* Oral nicotine pouches with an aftertaste? Part 2: in vitro toxicity in human gingival fibroblasts. *Arch Toxicol* **97**, 2343-2356 (2023). https://doi.org/10.1007/s00204-023-03554-9

30 Bielecki, T. & Dohan Ehrenfest, D. M. Platelet-rich plasma (PRP) and Platelet-Rich Fibrin (PRF): surgical adjuvants, preparations for in situ regenerative medicine and tools for tissue engineering. *Curr Pharm Biotechnol* **13**, 1121-1130 (2012). https://doi.org/10.2174/138920112800624292

31 Rebimbas Guerreiro, S. *et al.* Platelet-Rich Plasma and Platelet-Rich Fibrin in Endodontics: A Scoping Review. *Int J Mol Sci* **26** (2025). https://doi.org/10.3390/ijms26125479

32 Cho, E. B. *et al.* Effect of platelet-rich plasma on proliferation and migration in human dermal fibroblasts. *J Cosmet Dermatol* **18**, 1105-1112 (2019). https://doi.org/10.1111/jocd.12780

33 Taylor, L. M. & Khachigian, L. M. Induction of platelet-derived growth factor B-chain expression by transforming growth factor-beta involves transactivation by Smads. *J Biol Chem* **275**, 16709-16716 (2000). https://doi.org/10.1074/jbc.275.22.16709

34 Giarratana, A. O., Prendergast, C. M., Salvatore, M. M. & Capaccione, K. M. TGF-beta signaling: critical nexus of fibrogenesis and cancer. *J Transl Med* **22**, 594 (2024). https://doi.org/10.1186/s12967-024-05411-4

35 Mehrabani, D., Seghatchian, J. & Acker, J. P. Platelet rich plasma in treatment of musculoskeletal pathologies. *Transfus Apher Sci* **58**, 102675 (2019). https://doi.org/10.1016/j.transci.2019.102675

36 Li, C. X. *et al.* Inhibiting autophagy promotes collagen degradation by regulating matrix metalloproteinases in pancreatic stellate cells. *Life Sci* **208**, 276-283 (2018). https://doi.org/10.1016/j.lfs.2018.07.049

37 Gao, Y. *et al.* ATG5-regulated CCL2/MCP-1 production in myeloid cells selectively modulates anti-malarial CD4(+) Th1 responses. *Autophagy* **20**, 1398-1417 (2024). https://doi.org/10.1080/15548627.2024.2319512

38 Kolattukudy, P. E. & Niu, J. Inflammation, endoplasmic reticulum stress, autophagy, and the monocyte chemoattractant protein-1/CCR2 pathway. *Circ Res* **110**, 174-189 (2012). https://doi.org/10.1161/CIRCRESAHA.111.243212

39 Korhonen, E. *et al.* SQSTM1/p62 regulates the production of IL-8 and MCP-1 in IL-1beta-stimulated human retinal pigment epithelial cells. *Cytokine* **116**, 70-77 (2019). https://doi.org/10.1016/j.cyto.2018.12.015

40 An, Q., Yan, W., Zhao, Y. & Yu, K. Enhanced neutrophil autophagy and increased concentrations of IL-6, IL-8, IL-10 and MCP-1 in rheumatoid arthritis. *Int Immunopharmacol* **65**, 119-128 (2018). https://doi.org/10.1016/j.intimp.2018.09.011

41 Qin, B., Zhou, Z., He, J., Yan, C. & Ding, S. IL-6 Inhibits Starvation-induced Autophagy via the STAT3/Bcl-2 Signaling Pathway. *Sci Rep* **5**, 15701 (2015). https://doi.org/10.1038/srep15701

42 Festa, B. P. *et al.* Microglial-to-neuronal CCR5 signaling regulates autophagy in neurodegeneration. *Neuron* **111**, 2021-2037 e2012 (2023). https://doi.org/10.1016/j.neuron.2023.04.006

43 Zeng, Z., Lan, T., Wei, Y. & Wei, X. CCL5/CCR5 axis in human diseases and related treatments. *Genes Dis* **9**, 12-27 (2022). https://doi.org/10.1016/j.gendis.2021.08.004

44 Veriepe-Salerno, J. *et al.* MALT-1 shortens lifespan by inhibiting autophagy in the intestine of C. elegans. *Autophagy Rep* **2**, 2277584 (2023). https://doi.org/10.1080/27694127.2023.2277584

45 Fang, Y. & Svoboda, K. K. Nicotine inhibits myofibroblast differentiation in human gingival fibroblasts. *J Cell Biochem* **95**, 1108-1119 (2005). https://doi.org/10.1002/jcb.20473

46 Malhotra, R., Kapoor, A., Grover, V. & Kaushal, S. Nicotine and periodontal tissues. *J Indian Soc Periodontol* **14**, 72-79 (2010). https://doi.org/10.4103/0972-124X.65442

47 Giannelli, A. *et al.* Utilization of Platelet-Rich Plasma in Oral Surgery: A Systematic Review of the Literature. *J Clin Med* **14** (2025). https://doi.org/10.3390/jcm14082844

48 Gomri, F., Vischer, S., Turzi, A. & Berndt, S. Swiss Medical Devices for Autologous Regenerative Medicine: From Innovation to Clinical Validation. *Pharmaceutics* **14** (2022). https://doi.org/10.3390/pharmaceutics14081617

49 Omondi, R. O., Bellam, R., Ojwach, S. O., Jaganyi, D. & Fatokun, A. A. Palladium(II) complexes of tridentate bis(benzazole) ligands: Structural, substitution kinetics, DNA interactions and cytotoxicity studies. *Journal of inorganic biochemistry* **210**, 111156 (2020). https://doi.org/10.1016/j.jinorgbio.2020.111156
50 Thome, M. P. *et al.* Ratiometric analysis of Acridine Orange staining in the study of acidic organelles and autophagy. *J Cell Sci* **129**, 4622-4632 (2016). https://doi.org/10.1242/jcs.195057
51 Traganos, F. & Darzynkiewicz, Z. Lysosomal proton pump activity: supravital cell staining with acridine orange differentiates leukocyte subpopulations. *Methods Cell Biol* **41**, 185-194 (1994). https://doi.org/10.1016/s0091-679x(08)61717-3
52 T., S. in *Wormbook* 1-11 (2006).
53 Berndt, S. *et al.* Angiogenesis Is Differentially Modulated by Platelet-Derived Products. *Biomedicines* **9** (2021). https://doi.org/10.3390/biomedicines9030251

Acknowledgements

The *C. elegans* strains were kindly provided by the *C. elegans* Genetics Center (University of Minnesota, MN, USA). A great thanks to Nicolas Liaudet, who coded the script for picture quantification on QuPath and to the Bioimaging facility of the UNIGE for their help.
We thank Vanessa Fétaud Lapierre and Gaël Vieille for allowing us the use of the UFA facility and its equipment.

Author contributions

S.B. and C.G. designed the study. S.B, JA.C, performed the cell experiments. J.VS. designed and performed the experiments in *C. elegans*. A.T, M.C, S.V and C.G. contributed to the final version of the manuscript.

Data availability statement

All data generated or analyzed during this study are included in this published article.
Experiments were realized in accordance with ARRIVE guidelines.

Declaration of competing interest

The authors declare the following competing interest: S.B. is head project manager, cell therapy, at Regen Lab; S.V. is an employee by Regen Lab SA; and A.T. is the CEO of Regen Lab SA. The authors receive salary from Regen Lab SA. The study received financial support, materials and reagents from Regen Lab SA. Regen Lab SA develops and commercializes products in the field related to this study and could reasonably benefit from its findings. All other authors declare no competing interests.